Design and Implementation of Close-loop Detection for Coupled Core Fluxgate Magnetic Sensors

Jingjie Li, Yanzhang Wang, Jiaqing Shi, Hadi Heidari
Key Laboratory of Geophysical Exploration Equipment, Jilin University, China
Microelectronics Lab (meLAB), James Watt School of Engineering, University of Glasgow, G12 8QQ, UK

***Abstract*— This paper presents a closed-loop detection strategy with significant potential to solve the detection defects existed in the residence-times difference (RTD) method of the coupled core fluxgate magnetic sensors. The external magnetic field (e.g. Earth's magnetic field), as the main source of these detection defects, has been analyzed by the theoretical investigation. To overcome such deficiencies, the close-loop detection method based on the analog-type RTD readout method and magentic flux-balance detection is utilized to implement external magnetic field real-time compensation and achieve a near-zero-field working state of the magnetic material. The fluxgate with the optimized detection strategy and vertical arrangement structure has been designed, fabricated and examined, and the preliminary results showed steady operation and a detection resolution of ±0.10 nT. The optimized detection method based on the balance detection concept proposed in this manuscript demonstrated a great potential to obtain the optimal detection performances which are embedded in the coupling-induced oscillation of nonlinear dynamics.**

Keywords—magnetic sensors, closed-loop detection, field-compensation, optimal regime, performances enhancement

I. Introduction

Fluxgate magnetic sensor, is the best sensor for nano-Tesla field detection considering its low price, small dimension, high resolution, vector measruement, and robustness. It has been widely used to detect weak static magnetic fields at room temperature, and found applicability in many areas like biological magnetic detection, geophysical prospecting, space detection, and numerous other applications [1-5]. And it becomes the indispensable satellite payload in many aerospace magentic survey. The magnetic field detection can usually provide more real-time and direct information compared with the electric field sensing, and gains a lot of attractions in biosensing area. Due to the more complex and weak magentic field generated in the biosensing application especially for disease diagnose, the magnetic sensor need to have higher spatial resolution, compact size, and low power consumption while having excellent sensitivity and detection resolution [6-9].

The newly developed fluxgate magnetometer is base on the coupling induced oscillation in the soft magnetic material. This self-induced oscillation is originated from the Hopf bifurcation and heteroclinic cycle theory, and the prerequisite is the ring-coupling topology and proper initial statese [10-12]. The oscillation based on the nonlinear dynamics is ultra sensitive to the characteristic changes, and for the magnetic field detetcion it has great sensitibity [13-14].

According to our recent experiments, the sensor output linearity and sensitivity are constrained by the external magnetic field in the residence times difference (RTD) readout strategy[16]. And the frequency of the self-oscillation is also influenced by the external magnetic field, which makes injection locking (effective method to reduce noise floor) challenging to implement.

In this paper, we investigate these detection defects and their influences on sensor performances and provide a potential method to enhance sensor detection.

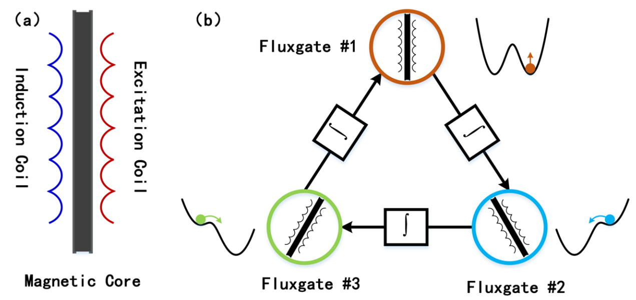

Fig. 1 Basic structure of CCFM. (a) Structure of the Fluxgate element; (b)Illustration of the CCFM.

II. Defects of Open-Loop RTD Detection in CCFM

The CCFM (shown in Fig. 1) is constructed by unidirectional ring coupling N (N=3 in our design) fluxgate elements with cyclic boundary condition. The theoretical analysis of the CCFM with RTD detection scheme has already been thoroughly studied by Bulsara A. R. et al. [12-15], and the detection defects caused by the nonzero magnetic field are analyzed based on the achieved theoretical analysis in this section. The induced nonlinearity and constrained sensitivity directly influence the sensor detection resolution, and the frequency changes make the injection locking lose the advantages.

A. Nonlinearity Influenced by Magnetic Field

The RTD is used as a quantifier of the target magnetic field in CCFM [12,15], given as

$$RTD=\frac{\pi}{\sqrt{c x_{\text{inf}}}}\left(\frac{1}{\sqrt{\lambda_c-\lambda}}-\frac{1}{\sqrt{\lambda_c-\lambda+2\varepsilon}}\right) \qquad (1)$$

where c is the system parameter governing nonlinearity (c>1 for the nonlinear system), $x_{\text{inf}}=[(c\text{-}1)/c]^{1/2}$ is the infection point of magnetic hysteresis, ε is the magnitude of the magnetic field, $\lambda_c=-\varepsilon-x_{\text{inf}}+c^{-1}\tanh^{-1}x_{\text{inf}}$ is the critical coupling strength, and λ is the coupling factor determined by the circuits.

Based on Eq. (1), the RTD responses with different magnetic fields are shown in Fig. 2. With the increase of the magnetic field, the output nonlinearity increases gradually. And with the coupling strength $|\lambda|$ decreases, the nonlinearity becomes more obvious while the sensor sensitivity increases.

Identify applicable funding agency here. If none, delete this text box.

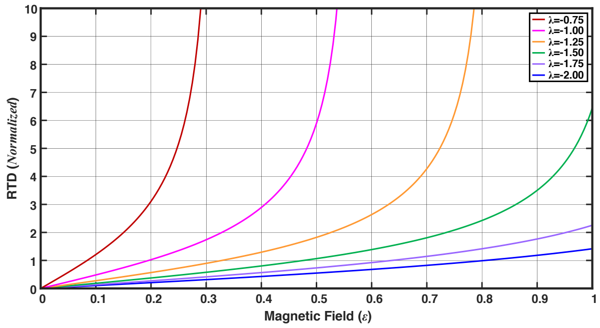

Fig. 2 The RTD responses with different magnetic fields (c=3).

B. *Sensitivity Constrained by Nonzero Magnetic Field*

The CCFM will immediately stop working as soon as its coupling-induced oscillation vanishes [12]. Based on this fact, the sensor measurement range can be determined by keeping this oscillation alive, that is

$$\varepsilon < c^{-1}\tanh^{-1} x_{\mathrm{inf}} - x_{\mathrm{inf}} - \lambda \tag{2}$$

The sensor sensitivity can be determined by the derivative of RTD with respect to magnetic field ε in the sensor's linear region. The measurement range and sensitivity are given in Fig. 3. With the coupling strength $|\lambda|$ decreases, the sensitivity increases while the measurement range decreases. That is, the sensitivity is constrained by the dynamic range/magnetic field.

C. *Frequency Changes with Nonzero Magnetic Field*

The oscillation frequency ω of CCFM [15] is given in Eq. (3) and the relationship between frequency and magnetic field under different coupling factor is shown in Fig. 4.

$$\omega = \frac{2\sqrt{cx_{\mathrm{inf}}}}{3}\left(\frac{\sqrt{(\lambda_c-\lambda)(\lambda_c-\lambda+2\varepsilon)}}{\sqrt{\lambda_c-\lambda}+\sqrt{\lambda_c-\lambda+2\varepsilon}}\right) \tag{4}$$

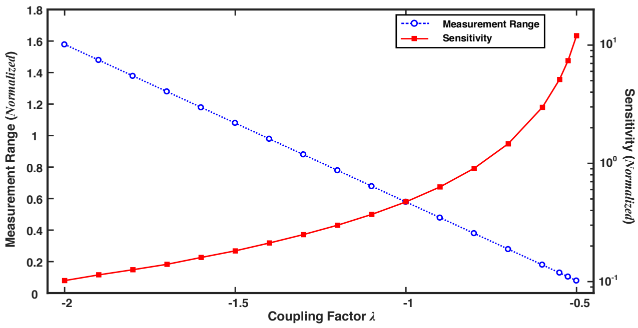

Fig. 3 The measurement range and sensitivity of CCFM (c=3).

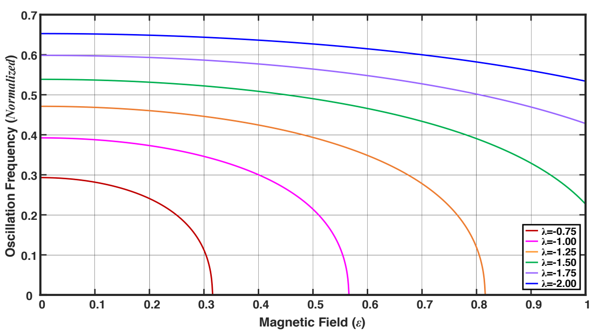

Fig. 4 The oscillation frequency vs. magnetic field (c=3).

As shown in Fig. 4, the oscillation frequency changes with the magnetic field, whatever the coupling factor is. And for the small coupling strength, the changes of oscillation frequency is particularly apparent.

III. Optimization Based on Feedback Technology

The nonzero magnetic field can give rise to output nonlinearity, sensitivity limitation, and frequency change. These undesired effects will cause sensor accuracy degradation [16] and increase the complexity of injection locking, which can effectively reduce the sensor noise floor [17,18] If the CCFM is working at a zero magnetic field during its operation, these degradations will vanish. Based on this fact, the feedback system with modified RTD detection method to achieve a zero magnetic field running regime of CCFM.

A. *Modification of RTD Detection Method*

The output of CCFM utilizing RTD detection strategy is pure digital [13], which makes it difficult to compatible with the voltage feedback unless employing DA (digital to analogue) converter. The RTD detection method has already optimized for single-core fluxgate magnetometer (SCFM) [16], here we modified it for CCFM to implement feedback detection using the same method as shown in Fig. 5. Integrating the oscillation signal $x(t)$ over one period, we can get

$$\begin{aligned} V &= \int_{t_{p1}}^{t_{p2}} x(t)dt \approx \int_{t_{p1}}^{t_{n1}} B_s dt + \int_{t_{n1}}^{t_{p2}} -B_s dt \\ &= \frac{B_s\pi}{\sqrt{cx_{\mathrm{inf}}}}\left(\frac{1}{\sqrt{\lambda_c-\lambda}} - \frac{1}{\sqrt{\lambda_c-\lambda+2\varepsilon}}\right) \end{aligned} \tag{5}$$

where V is the integration voltage output, t_{p1}, t_{n1}, t_{p2} represent the inflexion moments, B_s is the saturation induction of the magnetic core.

B. *Closed-loop Design of RTD Detection Method*

Fig. 6 shows the closed-loop structure of CCFM with feedback. The fluxgate elements are installed in a vertical arrangement for magnetic crosstalk suppression and probe miniaturization [19]. The CCFM probe contains three fluxgate elements which are coupled in a ring topology by the coupling circuits, and each fluxgate element consists of the magnetic core, excitation coil and induction coil. The three parts share the feedback and locking coils.

The detection circuits are modified according to the modification theory of RTD detection method. The circuits are composed of a low-pass filter, leaky integrator and feedback resistor basically. For bandwidth expanding, the

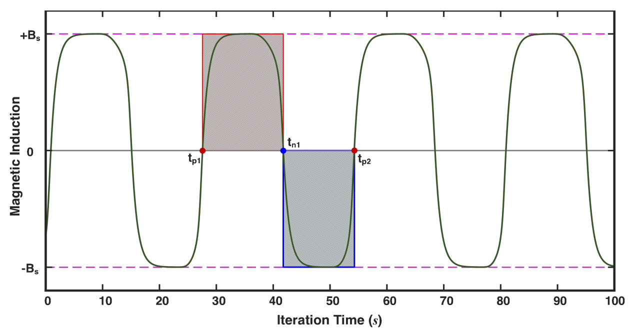

Fig. 5 The oscillation patterns of CCFM (c=3).

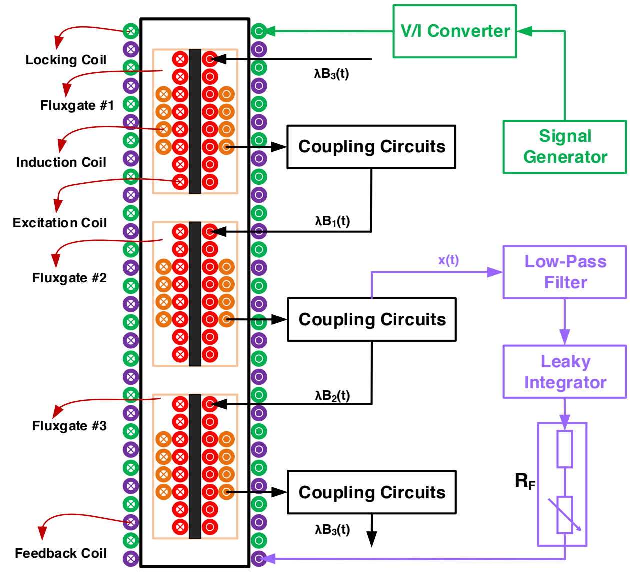

Fig. 6 The close-loop structure of CCFM with feedback.

circuits may need an amplifier for feedback enhancement. The detection circuits process the signal from the middle element for its more uniform distribution of feedback magnetic field. When the feedback system is balanced, the measurement output can be evaluated as,

$$V_{out} = \frac{L_F\left(R_F + R_{FC}\right)}{\mu_0 N_F} H_x \tag{6}$$

where L_F, N_F and R_{FC} are the coil length, the turns and the equivalent impedance of the feedback coil respectively, R_F is the feedback resistor.

C. *Feedback Benefits the Injection Locking*

The injection locking is implemented by a signal generator, a V/I (voltage to current) converter and the locking coil [17]. In addition, the locking function is triggered on by a time-delay signal to ensure the feedback system is stable. The injection frequency is set to be the same as the oscillation frequency. After the system reaches its equilibrium state, the frequency of the coupling-induced oscillation will be determined and remain unchanged. The oscillation frequency may change on a small scale due to the magnetic perturbation. However, once the injection locking enabled, the oscillation frequency will immediately follow the injection frequency and remain consistent.

IV. Implementation and Preliminary Experiments

In order to validate the close-loop detection for CCFM, the CCFM prototype has been implemented and tested, and the preliminary results will be given.

A. *Newly Designed CCFM Prototype*

The CCFM prototype is using the vertical arrangement structure to make the feedback detection and injection locking conveniently to implement, as shown in Fig. 7. The specific parameters of the CCFM probe are shown in Table. I. The Cobalt-based amorphous alloy (No. 2714A) makes the magnetic core which is protected by a dedicated glass tube, and the coils are made from the 0.1mm enameled copper wire, and finally the CCFM probe is protected by a non-conductive carbon fiber tube.

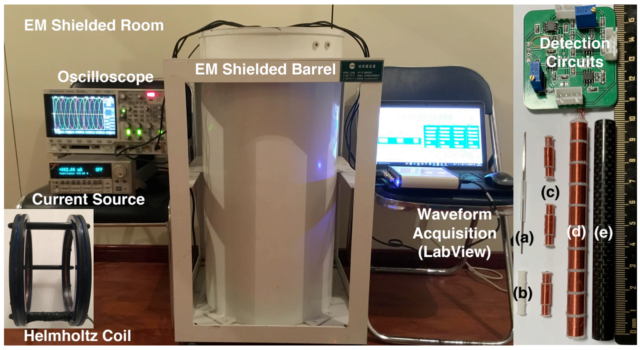

Fig. 7 The structure of the CCFM prototype and setup of the experiments. (a) Magnetic Core; (b) coil support; (c) fluxgate element; (d) CCFM probe; (e) probe protector.

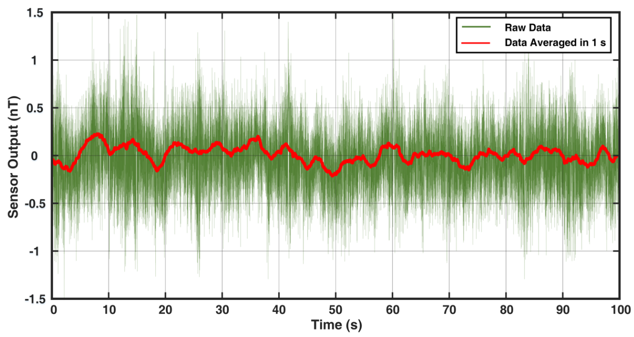

Fig. 8 The preliminary results of the close-loop CCFM.

B. *Experimental Environment and Results*

In order to provide a proper experimental environment for the evaluation of the performance of the newly designed fluxgate magnetometer, the electromagnetic (EM) shielded room, and a three-layer EM shielded barrel are employed. In the experiments, the EM shielded barrel is placed in the EM

TABLE I. Parameters Specification

Specification	Value
Coupling Parameters	
Elements Number	3 Fluxgate elements
Orientation Type	Vertical arrangement
Magnetic Material	Cobalt-based amorphous alloy ribbon
Mechanical Parts	
Support Structure	3D printing UV Curable Resin
Probe Protect Shell	Non-conductive carbon fiber
Excitation Coils	
Turns	200
Average Radius	1.5 mm
Induction Coils	
Turns	1000
Average Radius	2.0 mm
Feedback Coils	
Turns	2000
Average Radius	4.0 mm

shielded room, and the fluxgate probe is placed in the centre of the EM shielded barrel, as shown in Fig. 7. The shielding environment can provide a near-zero magnetic field environment with the remain magnetic field less than 0.1nT and a field noise less than 10pT, which is adequate for the fluxgate magnetic sensor calibration and testing.

The current source Keithley 6221 and a Helmholtz coil are utilized to generate the calibration magnetic field, and an oscilloscope DSOX2024A is employed to show the oscillation patterns, and the NI-DAQ USB4431 and driver inside LabView are used to capture the experimental data.

The preliminary results are shown in Fig. 8, the output fluctuation of the raw data is about ±1.0 nT, and the detection resolution can reach ±0.1 nT by a data averaging within 1 s.

V. Conclusion and Discussion

In this paper, the defects of RTD detection on CCFM are revealed by theoretical analysis, and the close-loop detection method based on feedback technology has been presented. The preliminary results show the close-loop detection have the potential to cope with the influences on CCFM caused by the nonzero magnetic field. The optimized detection method proposed in this paper demonstrated a great potential to achieve the optimal detection performances which are embedded in the coupling-induced oscillation of nonlinear dynamics.

The detailed parameters, including detection resolution, frequency response, and noise floor, should be investigated. After this, to further improve the detection performances, locking coupling-induced oscillation with different phases [18], controlling the sensitivity and range with an adaptive algorithm (PID or Kalman Filter), and adding magnetic compensation for excellent characterization will be explored in the future.

Acknowledgement

The research leading to this study under the funding from the Graduation Innovation Funding of Jilin University. The authors are also thankful to the China Scholarship Council for funding oversea research exchange in University of Glasgow (CSC NO. 201906170213).

References

[1] H. Heidari and V. Nabaei, Magnetic Sensors for Biomedical Applications. Wiley-IEEE Press, 2019.

[2] W. Magnes, and M. D. Michelena, “Future directions for magnetic sensors for space application,” IEEE Tran. Magn., vol. 45, no. 10, pp. 4493-4498, Oct. 2009.

[3] Z. Chu, H. Shi, M. J. PourhosseiniAsl, J. Wu, W. Shi, X. Gao, and et al, “A magnetoelectric flux gate: new approach for weak DC magnetic field detection,” Scientific Reports, vol. 7, no. 1, Aug. 2017.

[4] D. W. Lee, M. Eissa, A. Gabrys, B. Shulver, E. Mazotti, S. Lavangkul, and et al, “Fabrication and performance of integrated fluxgate for current sensing applications,” IEEE Tran. Magn., vol. 53, no. 11, Jun. 2017.

[5] M. Janosek, “Parallel Fluxgate Magnetometers,” in High Sensitivity Magnetometers, vol. II, A. Grosz, M. J. Haji-Sheikh, and S. C. Mukhopadhyay, Eds. Springer: Cham, 2017, pp. 41–61.

[6] H. Heidari, “Electronic skins with a global attraction,” Nature Electronics, vol. 1, no. 11, pp. 578-579, Nov. 2018.

[7] S. Zuo et al, "Integrated pico-tesla resolution magnetoresistive sensors for miniaturised magnetomyography," in 2020, .

[8] R. Das, F. Moradi and H. Heidari, "Biointegrated and Wirelessly Powered Implantable Brain Devices: A Review," IEEE Transactions on Biomedical Circuits and Systems, vol. 14, (2), pp. 1-1, 2020.

[9] S. Zuo et al, "Miniaturized magnetic sensors for implantable magnetomyography," 2020.

[10] M. Aguiar, P. Ashwin, A. Dias, and M. Field, “Dynamics of coupled cell networks: synchrony, heteroclinic cycles and inflation,” Journal of Nonlinear Science, vol. 21, no. 2, pp. 271-323, Nov. 2011.

[11] A. Palacios, V. In, and P. Longhini, “Symmetry-breaking as a paradigm to design highly-sensitive sensor systems,” Symmetry, vol. 7, no. 2, pp. 1122-1150, Jan. 2015.

[12] A. R. Bulsara, V. In, A. Kho, P. Longhini, A. Palacios, W. -J. Rappel, and et al, “Emergent oscillations in unidirectionally coupled overdamped bistable systems,” Physical Review E, vol. 70, no. 3, Sep. 2004.

[13] B. Ando, S. Baglio, A. R. Bulsara, and S. Vincenzo, “Residence times difference fluxgate magnetometers,” IEEE Sens. J., vol. 5, no. 5, pp. 895–904, Oct. 2005.

[14] A. R. Bulsara, J. F. Lindner, V. In, A. Kho, S. Baglio, V. Sacco, and et al, “Coupling-induced cooperative behaviour in dynamic ferromagnetic cores in the presence of a noise floor,” Phys. Lett. A, vol. 353, no. 1, pp. 4–10, 2006.

[15] A. R. Bulsara, V. In, A. Kho, A. Palacios, P. Longhini, J. Neff, and et al, “Exploiting nonlinear dynamics in a coupled-core fluxgate magnetometer,” Measurement Science and Technology, vol. 19, no. 7, Jun. 2008.

[16] J. Li, X. Zhang, J. Shi, H. Heidari, and Y. Wang, “Performance Degradation Effect Countermeasures in Residence Times Difference (RTD) Fluxgate Magnetic Sensors,” IEEE Sensors Journal, in press, 2019.

[17] B. Andò, S. Baglio, C. Trigona, A.R. Bulsara, N.G. Stocks, and A. Nikitin, “Injection-locking benefits for weak AC magnetic field detection in coupled-core fluxgate magnetometers,” IEEE International Instrumentation and Measurement Technology Conference Proceedings, 2012.

[18] F. Antoci, B. Andò, C. Trigona, A. R. Bulsara, A. Nikitin, N.G. Stocks, and et al, “Injection locking in coupled core fluxgate magnetometers: Exploiting nonlinearity to enhance sensitivity to weak, low frequency, target magnetic fields,” IEEE Sensors J., vol. 14, no. 2, pp. 554-562, Feb. 2014.

[19] Li, Jingjie, et al. "Magnetic Crosstalk Suppression and Probe Miniaturization of Coupled Core Fluxgate Sensors." 2019 IEEE SENSORS. IEEE, 2019.